

P. Innocente et al

Real-Time Fringe Correction Algorithm for the JET Interferometer

Real-Time Fringe Correction Algorithm for the JET Interferometer

P. Innocente¹, D. Mazon², E. Joffrin², M. Riva³

¹*Consorzio RFX – Corso Stati Uniti, 4 – 35127 Padova, Italy*

²*Association Euratom-CEA, CEA Cadarache, F-13108, St Paul lez Durance, France*

³*Associazione Euratom-ENEA sulla Fusione, C.R. Frascati, 00044 Frascati, Italy*

“This document is intended for publication in the open literature. It is made available on the understanding that it may not be further circulated and extracts or references may not be published prior to publication of the original when applicable, or without the consent of the Publications Officer, EFDA, Culham Science Centre, Abingdon, Oxon, OX14 3DB, UK.”

“Enquiries about Copyright and reproduction should be addressed to the Publications Officer, EFDA, Culham Science Centre, Abingdon, Oxon, OX14 3DB, UK.”

ABSTRACT

On the JET facility, the line-integrated electron density is measured by a multichannel far-infrared (FIR) interferometer. The basic source of radiation is a deuterium cyanide (DCN) laser ($\lambda=195\ \mu\text{m}$) measuring the density along four vertical and four lateral channels. During high-density discharge the system suffers from fringe jumps that are manually partially corrected by an off-line program. This intermittent phenomenon prevents reliable usage of the measured line-integrated density in a real-time feedback controller. To solve this problem we have developed a method to correct on the lateral channels in real-time the fringe jumps. The method uses the additional Alcohol laser ($\lambda=118.8\ \mu\text{m}$) interferometer present on the lateral channels to compensate the vibrations. The method has been successfully tested with off-line test data, before implementation on a VME system for the real time control of the JET discharges..

ABSTRACT

On the JET facility, the line-integrated electron density is measured by a multichannel far-infrared (FIR) interferometer. The basic source of radiation is a deuterium cyanide (DCN) laser ($\lambda=195\ \mu\text{m}$) measuring the density along four vertical and four lateral channels. During high-density discharge the system suffers from fringe jumps that are manually partially corrected by an off-line program. This intermittent phenomenon prevents reliable usage of the measured line-integrated density in a real-time feedback controller. To solve this problem we have developed a method to correct on the lateral channels in real-time the fringe jumps. The method uses the additional Alcohol laser ($\lambda=118.8\ \mu\text{m}$) interferometer present on the lateral channels to compensate the vibrations. The method has been successfully tested with off-line test data, before implementation on a VME system for the real time control of the JET discharges.

I. INTRODUCTION

Real-time control of the plasma behaviour requires many high reliable profile measurements. In particular, for profile control, multi chords (multi points) diagnostics, with a good space and time resolution, have to be used. For example real time profile control will be required to achieve steady state advanced confinement regimes. Transient confinement improvement has been observed in several Tokamaks (JET [1] and Tore Supra [2] in Europe, TFTR [3] and DIII-D [4] in USA and JT-60U [5] in Japan), in high performance regimes in which an Internal Transport Barrier (ITB) appears. The real-time control by feedback loops of plasma quantities such as the current density and the pressure profiles is required to maintain the high performance regimes in steady state, this it is important for the continuous operation of a fusion reactor.

One key measurement is the density profile, measured in JET by a multi-channel interferometer-polarimeter [6]. The system provides in real-time line-integrated measurements along four vertical and four lateral channels (see fig. 1). The interferometer measurements are subject to fringe jumps, as a consequence of some plasma events such as ELMs [7], fast density increases and disruptions [8] or pellet injection. Although off-line programs are able to correct most of the fringe jumps, their occurrence prevents the direct use of interferometric signals in a real-time feedback scheme. For that reason a real-time code has been developed to detect and correct the fringe jump events for the lateral channels of the JET interferometer.

After a brief introduction to the JET FIR interferometer (section II), the fringe jump characteristics are described in section III of this paper. The phase computation and the fringe jump correction method are given in section IV. Finally in section V, we describe the implementation of the correction method for the JET measurements and the tests performed on data to check its reliability.

II. THE INTERFEROMETER SYSTEM

The JET interferometer/polarimeter [6] performs the line-integrated density measurement 4 vertical and 4 nearly horizontal lateral channels (fig. 1).

Since all the mirrors of the vertical channels are installed on a vibration isolated C frame (tower), a mechanical structure able to keep to a low level the mirrors movement, the vertical channels use only a DCN laser ($\lambda = 195 \mu\text{m}$) for the line-integrated density measurement. In the lateral channels use in-vessel mirrors to reflect the beams back and therefore suffer from large path length variation. This makes necessary the use of a compensated interferometer that features a second wavelength interferometer Alcohol laser ($\lambda=118.8 \mu\text{m}$) for path length correction. In the following part we present in more detail the lateral channel set-up, together with the JET real-time computation of the line-integrated density. In fig. 2 the logical diagram for the lateral channels is sketched. A fraction of the DCN laser beam is frequency shifted by a rotating grating to produce a 100 kHz modulated interference signal for a heterodyne detection. A part of the Alcohol laser beam is frequency shifted by 5 kHz by the same method. The shifted and unshifted parts of both lasers are then combined together in such a way that both wavelengths share the same optical paths up to the detectors. After the detector (and preamplifier) a low-pass (0-30 kHz) and a non-overlapping (60-140 kHz) band-pass filter separate the two signals at 5 and 100 kHz. The signals are then supplied to the real time density computation VME system [9]. Inside the VME system, first the UXD5 module digitises the signal at 400 kHz and then a Motorola TMS320C40 (commonly known as a 'C40) DSP (Digital Signal Processor) computes the phase. The DCN and Alcohol phases are computed by the 'C40 in two different ways to account for the different modulation frequencies.

Concerning the DCN phase, samples arriving from the UXD5 module are treated in groups of four (s_1, s_2, s_3, s_4) and subtracted to get the (x,y) pair:

$$x = s_1 - s_3$$

$$y = s_2 - s_4$$

finally the phase, ϕ , in the $[-\pi, +\pi]$ range and the signal amplitude, A, are computed by the relations:

$$x = 2A\cos(\phi)$$

$$y = 2A\sin(\phi)$$

The DCN phase is then computed each 0.1 msec recording only one phase every 10 phase evaluations. For the Alcohol phase the samples are treated in groups of forty by convoluting the half 5 kHz cycle with a fixed half-cycle cosine and sine wave:

$$v_1 = \frac{\sqrt{2}}{40} \sum_{i=1}^{40} s_i \cos\left(\frac{\pi}{40}i\right)$$

$$v_2 = \frac{\sqrt{2}}{40} \sum_{i=1}^{40} s_i \sin\left(\frac{\pi}{40}i\right)$$

$$v_3 = \frac{\sqrt{2}}{40} \sum_{i=1}^{40} s_{i+40} \cos\left(\frac{\pi}{40}i\right)$$

$$v_4 = \frac{\sqrt{2}}{40} \sum_{i=1}^{40} s_{i+40} \sin\left(\frac{\pi}{40}i\right)$$

and again, as for the DCN signal, v_1, v_2, v_3, v_4 are combined to get a (x,y) pair:

$$x = v_1 - v_3$$

$$y = v_2 - v_4$$

from which the phase is computed every 100 μsec by halfcycle overlapping the 200 μsec (5 kHz) intervals.

For both lasers, the phase is kept constant when the amplitude becomes lower than a pre-set threshold. By that method the phase is implicitly computed relatively to a nominal 100 kHz signal for the DCN laser (5 kHz for the Alcohol laser) both for the measurements channels and the references channels. Since the frequency modulation obtained by the rotating grating can drift away from 100 kHz (5 kHz) by $\pm 1\%$, to get the right phase variation from the plasma, the reference phase is subtracted from the channels measurement phase.

By this, and any other possible, method the phase computed from the measured signals is obtained in the $[-\pi, +\pi]$ range, then the total phase variation, ψ , is computed summing the fringe number, F , multiplied by 2π .

$$\psi = \phi + 2\pi F$$

To get the fringe number, ϕ is followed to identify the time when F has to be increased (or decreased) by one. When for any reason, for example a too large total phase variation between two phase evaluations, the fringe number is wrong evaluated the total phase is also affected. Such events are usually called fringe jumps and they introduce an error on the total phase evaluation equal to an integer number multiplied by 2π .

In the JET system once the total phase is computed the result is stored, for off-line analysis, with a maximum time resolution of 0.5 ms. The signal is also available in real-time, but still requires correction of fringe jumps.

The above method, which we will call in the following the “4-points method”, is very fast in computing the phase with high precision and presents the advantage of being insensitive to a signal offset. But three main problems remain:

- 1) The phase is computed correctly only for signals with a frequency not too far from the nominal frequencies;
- 2) It needs a nearly constant signal amplitude during one modulation period;
- 3) It can loose fringes when the phase is keep constant during the low amplitude intervals and the modulation frequency is far from the nominal one.

An example of a good measurement performed on four of the eight channels of the interferometer is shown in fig.3a, whereas in fig. 3b display a case with many fringe jumps (in the grey time interval). In that last case, the presence of fringe jumps is shown by the non-zero value of the line-integrated density after the end of the shot on both the vertical and lateral channels.

III. FRINGE JUMP DETECTION AND CHARACTERISTICS

In a compensated interferometer the presence of fringe jump events can be systematically detected by analysing the time evolution of the path length variation. In the following for simplicity we will

call vibrations the path length variations although a small part only of the path length variation has a periodic behaviour.

Ignoring effects different from vibrations and density (as for example phase measurement errors due to electronic noise), the phase measurement of the two wavelengths of a compensated interferometer can be written in the following way:

$$\psi_1 = K\lambda_1 \int n \, dl + 2\pi \frac{V}{\lambda_1} \quad (1a)$$

$$\psi_2 = K\lambda_2 \int n \, dl + 2\pi \frac{V}{\lambda_2} \quad (1b)$$

where λ_1 , and λ_2 are the main and compensation wavelengths, while K is a constant equal to:

$$K = \frac{e^2}{4\pi c^2 \epsilon_0 m_e} = 2.82 \cdot 10^{-15} [m]$$

Multiplying equations (1a) and (1b) respectively by λ_1 and λ_2 and then taking the difference, it is possible to obtain the line-integrated density and vibrations amplitude:

$$\int n \, dl = \frac{1}{K} \cdot \frac{\lambda_1 \psi_1 - \lambda_2 \psi_2}{\lambda_1^2 - \lambda_2^2} \quad (2a)$$

$$V = \frac{1}{2\pi} \cdot \frac{\frac{\psi_2}{\lambda_2} - \frac{\psi_1}{\lambda_1}}{\frac{1}{\lambda_2^2} - \frac{1}{\lambda_1^2}} \quad (2b)$$

For convenience the vibration amplitude can be normalised to one of the two wavelengths (or in other word expressed in fraction of fringes). In the following examples we will always plot the vibrations normalised to the DCN wavelength:

$$\bar{V} = \frac{1}{2\pi\lambda_1} \cdot \frac{\frac{\psi_2}{\lambda_2} - \frac{\psi_1}{\lambda_1}}{\frac{1}{\lambda_2^2} - \frac{1}{\lambda_1^2}} \quad (2c)$$

Looking to the normalised vibrations amplitude signal, the fringe jumps can be easily seen as a fast large variation (fig. 4). For DCN fringe jumps alone the variation is close to an integer number (fig. 4b) while for Alcohol fringe jumps the variation is close to an integer number multiply by $\lambda_{\text{Alcohol}}/\lambda_{\text{DCN}} \cong 0.61$ (fig. 4a). When both DCN and Alcohol fringe jumps are present the variation can assume any value.

To understand the origin of the fringe jumps problem, all analogical signals needed to compute the line-integrated density on one of the lateral channels have been fast sampled and recorded at 1 MHz. To have a complete set of data the signals have been recorded in the points B, C of fig. 2. for channel 5 and the reference channel. Furthermore, to understand the possible effect of the filters the signal at point A of channel 5 has been also recorded.

Initially the fast sampled signals have been analysed to see what happens when the fringe jumps are observed on the phase measurements. The channel 5 fast measurements signals during fringe jumps events show an amplitude (fig. 5b, 5d) dropping close to zero in agreement with the amplitude computed by the real time VME system (fig. 5a, 5c). Furthermore it appears that the Alcohol signal can, in some situations, be larger than zero, but far from a 5 kHz wave. As we see in fig. 6, during the two grey intervals the amplitude of the Alcohol signal is not small but the signal is completely different from a single harmonic 5 kHz wave. In those conditions any method used to compute the phase produces an erroneous result, while the computed amplitude can appear larger than zero. Thus it is not possible to use the amplitude signal as a good indicator of a correct phase evaluation. It has to be mentioned that in all the cases during the same time intervals, the reference channel signals do not show any notable amplitude variation, confirming that the jumps are due to transient processes in the plasma.

The signal recorder in point A (before the filters) showed the same phenomenon, confirming that the problem is caused by the plasma acting as to reduce and modulate the amplitude of the interference signals. In most of the cases the amplitude is reduced in presence of events associated to local density gradient build up (like during ELMs) or fast density variation (like during disruptions or pellets injection). In the first case the problem seems to be due to a diffraction effect, while for the second it seems to be due to the too slow frequency modulation, although only in a few cases this was confirmed by the fast sampled signals.

IV. FRINGE JUMPS CORRECTION AND PHASE COMPUTATION METHOD

To correct the fringe jumps a method has been investigated based on the simultaneous DCN and Alcohol phase measurements available for the lateral channels. In particular the applicability of a technique like the one used in Tore Supra [10,11] has been analysed. Before discussing its applicability to the JET case, a brief description of the method is reported below.

The phase variation between two consecutive time samples can be written in the following way:

$$\Delta\phi_1 + 2\pi\Delta F_1 - \frac{2\pi\Delta V}{\lambda_1} = K\lambda_1\Delta \int n dl \quad (3a)$$

$$\Delta\phi_2 + 2\pi\Delta F_2 - \frac{2\pi\Delta V}{\lambda_2} = K\lambda_2\Delta \int n dl \quad (3b)$$

Where $\Delta\phi$ is the phase variation in the range $[-2\pi, 2\pi]$ while ΔF is the number of fringe variation. Dividing by λ the two equations it is possible to find the relation:

$$\Delta F_1 = \left(\frac{\Delta\phi_2}{2\pi} + \Delta F_2 \right) \frac{\lambda_1}{\lambda_2} - \frac{\Delta\phi_1}{2\pi} - \frac{\Delta V}{\lambda_1} \left[\left(\frac{\lambda_1}{\lambda_2} \right)^2 - 1 \right] \quad (4)$$

For long wavelengths interferometers (typically FIR), on short time interval the phase variation due to the vibrations variation, ΔV , is usually very small, while during the same time interval the phase variation due to the density can be large. More quantitatively the phase can change by more

than a fringe ($|\Delta F| > 1$) during a sampling time interval while the phase variation due to the vibrations is typically a small fraction of a fringe ($|\Delta V/\lambda| \ll 1$). Neglecting the vibrations part the relation (4) becomes:

$$\Delta F_1 = \left(\frac{\Delta\phi_2}{2\pi} + \Delta F_2 \right) \frac{\lambda_1}{\lambda_2} - \frac{\Delta\phi_1}{2\pi} \quad (5)$$

In this relation there are two unknowns: ΔF_1 and ΔF_2 but since they are integer numbers they can be found interactively starting from $\Delta F_2 = 0$ and increasing/decreasing ΔF_2 up to the point when ΔF_1 is close to a natural number in relation (5). The maximum allowed error, ϵ_{\max} , (difference between ΔF_1 and the closest natural number) depends on what is the maximum expected phase variation, between the two sampled points, due to vibrations and measurement errors. The smaller ϵ_{\max} , the higher is the probability of getting the right calculated values for ΔF_1 and ΔF_2 .

The previous statement can be better expressed going back to relation (4) written in the following way:

$$\Delta F_1 = \Delta F_2 \frac{\lambda_1}{\lambda_2} + \left(\frac{\Delta\phi_2}{2\pi} \frac{\lambda_1}{\lambda_2} - \frac{\Delta\phi_1}{2\pi} \right) + \frac{\Delta V}{\lambda_1} \left[\left(\frac{\lambda_1}{\lambda_2} \right)^2 - 1 \right] \quad (6)$$

for a generic F_2 the right part of the previous expression can be expressed as:

$$F_1 + f_1 + \left(\frac{\Delta\phi_2}{2\pi} \frac{\lambda_1}{\lambda_2} - \frac{\Delta\phi_1}{2\pi} \right) + \frac{\Delta V}{\lambda_1} \left[\left(\frac{\lambda_1}{\lambda_2} \right)^2 - 1 \right] \quad (7)$$

where F_1 is an integer number $F_1 = \text{NINT} \left(F_2 \frac{\lambda_1}{\lambda_2} \right)$, and f_1 is the fractional part $f_1 = F_2 \frac{\lambda_1}{\lambda_2} - F_1$. When $F_2 = \Delta F_2$ the fractional part becomes:

$$f_1 = - \left(\frac{\Delta\phi_2}{2\pi} \frac{\lambda_1}{\lambda_2} - \frac{\Delta\phi_1}{2\pi} \right)$$

and the right term of equation (6) reduces to:

$$\Delta F_1 + \frac{\Delta V}{\lambda_1} \left[\left(\frac{\lambda_1}{\lambda_2} \right)^2 - 1 \right]$$

showing how the vibrations prevent getting an exact integer number, requiring a maximum error to be defined:

$$\epsilon_{\max} = \frac{\Delta V_{\max}}{\lambda_1} \left[\left(\frac{\lambda_1}{\lambda_2} \right)^2 - 1 \right]$$

Unfortunately the vibration amplitude not only determines ϵ_{\max} , but can also lead to choosing a wrong couple of fringe numbers $[F_1, F_2]$. This happens when the vibration amplitude reduces to less than $\Delta F_1 = \left(\frac{\Delta\phi_2}{2\pi} + \Delta F_2 \right) \frac{\lambda_1}{\lambda_2} - \frac{\Delta\phi_1}{2\pi} - \epsilon_{\max}$ the last three terms of relation (7). The probability to find a wrong couple $[F_1, F_2]$ depends not only on the vibration amplitude but also on the wavelength ratio and the maximum allowed number of fringe jumps. That can be seen by computing F_1 and f_1 in function of F_2 and then sorting (F_1, F_2, f_1) in function of f_1 . It is simple to recognise that the vibrations easier could act to find a wrong couple where it is smaller the difference between the

various f_1 . In our case for the DCN and Alcohol lasers we find that varying F_2 from -5 to +5 the computed f_1 are nearly equally spaced with a difference, Δf , of about 0.08. Reducing the F_2 range only improve the separation of some of f_1 values (Tab. 1a). As an example from Tab. 1a it is possible to see that when ϵ_{\max} is larger than 0.04, searching the right couple [-3,-2] starting from F_2 from 0 going up to ± 2 leads to the erroneous choice of couple [2,1].

The previous analysis shown that we can check the applicability of the correction method comparing the measured vibrations variation between two consecutive sampling times, $\Delta \bar{V} = \bar{V}(t_{i+1}) - \bar{V}(t_i)$, to the Δf_1 values.

The calculation was initially done using the VME stored signals during the 0.5 msec sampling time intervals, but unfortunately the data produced a mean value of about ± 0.2 fringes (fig. 7a), which is incompatible with the correction method. In principle such large values could be due to large vibration amplitudes during the long sampling time or to the poor VME system computational precision.

To understand the origin of the value of \bar{V} we computed the phases directly from the fast sampled signals with the 4-points method, that allows getting the phase with a better time resolution (0.1 msec) and a good computation precision. It was found a $\Delta \bar{V}$ of the order of ± 0.03 fringes that is much smaller than what was obtained from the stored phase signals. It appears also that the lower value obtained from the fast sampled signals was not only due to the smaller time delay between points. From the off-line computed phase signals, computing the $\Delta \bar{V}$ between points with a sampling rate of 1 msec, the difference was still smaller than what obtained from the stored signals (fig. 7c), which demonstrates the poor computational precision affecting the existing VME system. The computation precision was finally improved by averaging the 10 DCN phase evaluation performed during the 0.1 msec. With this method a lower vibrations amplitude variation, corresponding to about ± 0.02 fringes (for the 0.1 msec time delay), was obtained (fig. 7b). Multiplying the last found value by the factor multiplying in relation (4) an effective vibrations variation of about ± 0.03 is found which is less than half the minimum Δf_1 .

The result obtained by computing the phase directly, indicates that the time evolution of the vibration is really slow in JET as needed by the correction method, but it is necessary to compute directly the phase from the raw signals.

Before implementing the correction method we also tried to investigate other phase computation methods to find a new one less affected by fringe jumps. To avoid the problems of the 4-points method, a method similar to the one used for analogical phase measurement devices was tested. That method computes the phase from the time delay between the zero crossings of the measured signal relatively to the reference signal. The method produced the expected result: the phase evaluation was noisier than the 4-points phase evaluation while presenting fewer fringe jumps in the case of long time interval, low amplitude signals. Although the method could be improved to reduce the noise, the frequency of events in which the method allows a reduction of fringe jump is very small in the present interferometer set-up. For these reasons the improved 4-points method was selected as the phase computation method for the correction algorithm.

V. DEVELOPMENT OF THE FRINGE JUMPS DETECTION AND CORRECTION METHOD

As we described previously at the end of section III, the fringe loss is mostly due to a low amplitude signal, but in some conditions the phase errors can also arise when the signal amplitude is not negligible. We will call “dark” the time interval of such phenomenon. This means that the correction method cannot be applied systematically between two consecutive points, but has to be used between points before and after the “dark” interval. This is different from the Tore Supra case where, since the fringe losses are only due to the slow computation speed, the method can be applied between all adjacent points. Hence to correctly apply the method two conditions have to be fulfilled: the start and end time of the “dark” interval have to be detected correctly, the vibrations during the “dark” interval has to be small.

Because the computed amplitude is not a good indicator of the reliability of the phase evaluation, we chose a different approach to detect the data points inside “dark” intervals. We considered that a point is part of a “dark” interval if we find a σ larger than a threshold. The method has the advantage that a wrong phase evaluation on any of the two lasers is automatically detected. The threshold value has to be set slightly larger than the typical σ . The smaller is the threshold, the better is the sensitivity to “dark” events. That again shows the importance of a good phase evaluation since it allows the use of smaller threshold values.

A statistical analysis of more than 300 shots presenting fringe jump events has been analysed, focussing on the behaviour of the vibration amplitude signal during the dark intervals.

For the typical ELMs events the “dark” interval last for about 1-2 msec. The corresponding variation caused by vibrations during this time interval are less than 0.1 fringes (fig. 7c). For discharge disruptions events the “dark” interval is very long and the vibrations amplitude exceeds one fringe. The statistical analysis suggests us to implement a three steps correction method. First from the phases computed by the improved 4-points method the “dark” intervals are identified on the basis of the σ value. Then, σ is computed between the first and last point outside the “dark” intervals and checked for a fringe jump. Finally, only if a fringe jumps is detected, the method uses the relation 4b) to adjust the fringe count at the end of the “dark” interval.

To have an accurate check of the ability of the method to correct all the fringe jumps, it would be necessary to apply it for the complete discharge duration, checking if the density returns close to zero after the end of the discharge. Such a procedure is not possible with the data recorded for some part of the discharge, as it was in our case. Only a qualitative indication of the method reliability has been obtained comparing the corrected density to the original one for the fringe jumps events found inside the fast measurements time windows.

As expected, looking to the corrected vibrations and line-integrated density time evolution, the method seems able to correct the fringe jumps during the ELM events (grey interval, figs. 8a, 8b). Instead the method is unable to correct the fringe jumps for the long disruption event (grey shadow intervals figs 8c, 8d) and it introduces some artificial vibrations reduction during the post disruption phase characterised by large vibrations (grey hatched intervals figs 8c, 8d).

A more precise indication of the method ability to correct the fringe jumps will be possible when the, now developing, real time system will correct the density for a large number of discharges.

VI. CONCLUSIONS AND FUTURE WORK

We analysed the line-integrated density measurement performed by the FIR interferometer at JET to solve the fringe jumps problem that prevents a real-time use of the measured density. We found that the fringe jumps are due to transient phenomena affecting the plasma density, which reduce and modulates the interference signals of the beams crossing the plasma section. For the lateral channels we developed a method able to correct most of the fringe jumps based on the simultaneous phase measurements at two wavelengths. For this purpose first we improved the phase computation method already used on the JET real-time system and developed a method to detect the occurrence of the fringe jump events. We are now testing a VME system for the lateral channels that will use a Power PC CPUs to compute the phase in real-time, detecting the fringe jumps and correcting them. As for the future work, based on the results we will get in a large number of discharges we plan to optimise the correction method reducing the effect of the vibrations in causing a wrong fringe number evaluation. For such purpose we considered two solutions. The vibrations present during the “dark” intervals can partially be subtracted by inferring them from the previously measured vibrations. A larger ϵ_{\max} (see section IV) could be allowed changing the wavelengths ratio, indeed using a different DCN emitting line ($\lambda=190 \mu\text{m}$) it is possible to use an ϵ_{\max} large up to 0.01.

REFERENCES

- [1]. JET Team 1997 Proc. 16th Int. Conf. on Fusion. Energy, IAEA, Montreal, Vol.I 487
- [2]. Equipe Tore Supra 1996, presented by X.Litaudon, Plasma Phys.Control.Fusion, **38** A251
- [3]. M..Bell et al., 1999 Plasma Phys. and Control.Fusion, **41**, A719
- [4]. E. J. Strait et al., 1995 Phys. Rev. Lett. **75** 4421
- [5]. T. Fujita et al., 1997 Proc. 16th Int. Conf. on Fusion Energy, IAEA, Montreal, Vol. I 227
- [6]. G. Braithwaite, et al, Rev. Sci. Instrum. **60**, 2825 (1989)
- [7]. G.Saibene and al submitted in PPCF
- [8]. Gill.R.D and al Nuclear Fusion Vol. 40 N 2, 163 (2000)
- [9]. H.E. Clarke,†“The Control of the Diagnostic KG1”, JDN/H(97)39
- [10]. C. Gil, “Calcul en temps reel del la densite lineique pour l’injection de gaz”, Tore Supra, NT $\phi/ n\infty 97$, September 1994.
- [11]. J.L. Bruneau, C. Gil,“Submillimetric interferometry of Tore Supra Plasma” in 14th Int. Conf. On Infrared and Millimeter Waves, W ,rzburg, October 1989

F_1	F_2	f_1	Δf_1
2	1	-0.36	0.08
-3	-2	-0.28	0.28
0	0	0.00	—
3	2	0.28	0.28
-2	-1	0.36	0.08

Table. 1a. Fraction of fringe variation for $\lambda_1=195\mu\text{m}$ and $\lambda_2=118.8\mu\text{m}$.

II. The interferometer

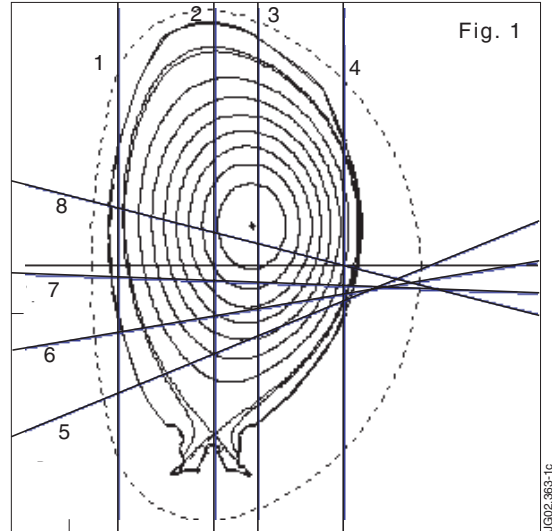


Figure 1: Interferometer channels position

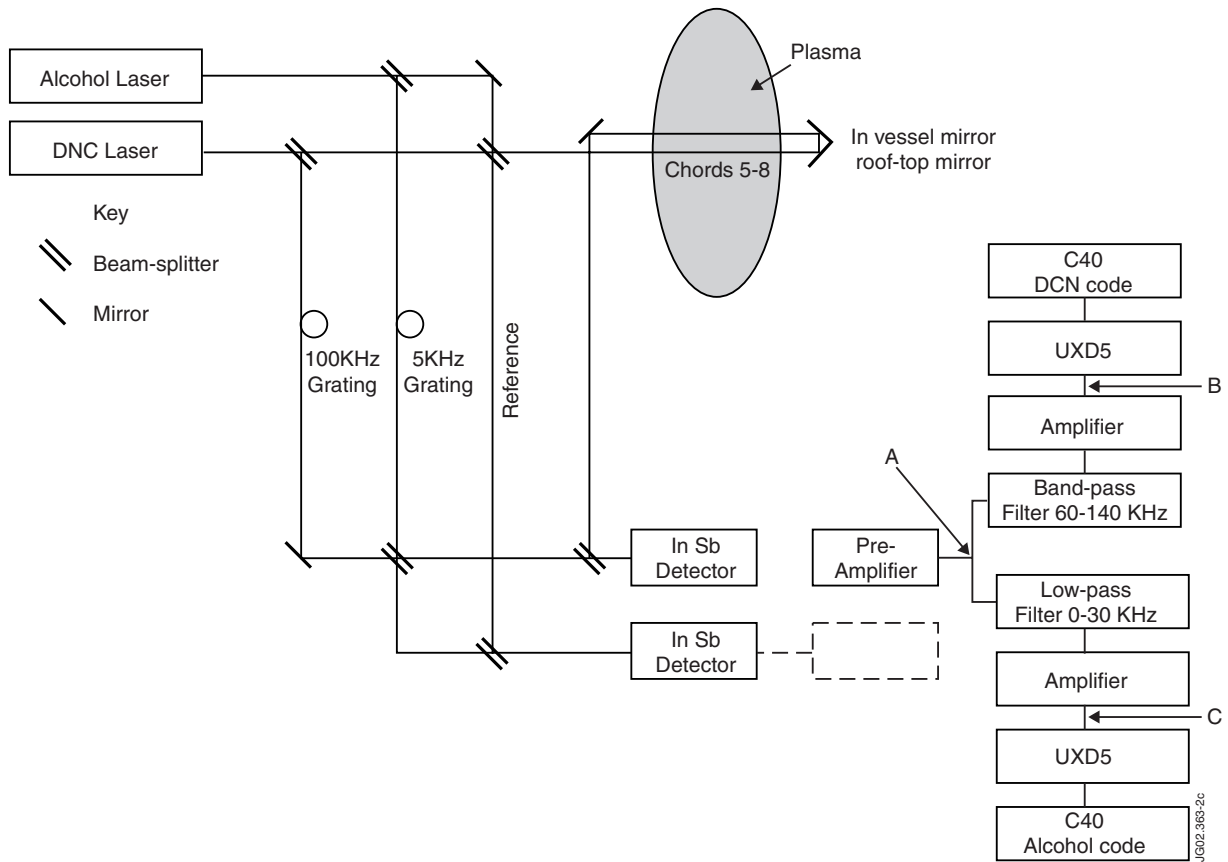


Figure 2: Diagram of the interferometer lateral channels

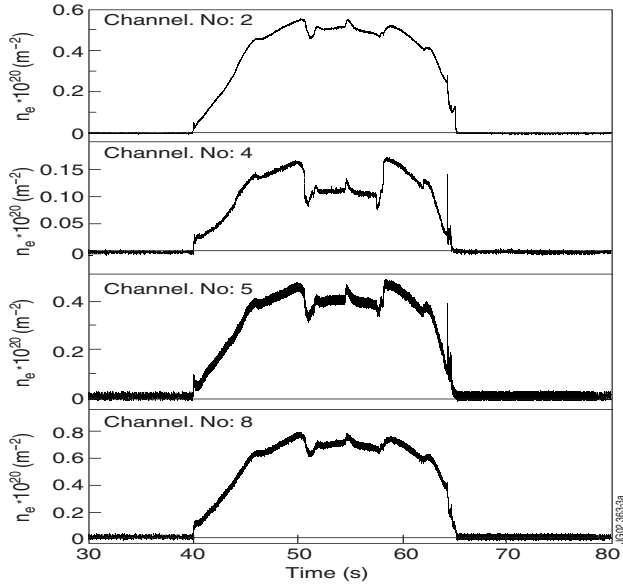


Figure 3a: Pulse No: 52832: Electron line integral measurements on channels #2, #4, #5, #8.

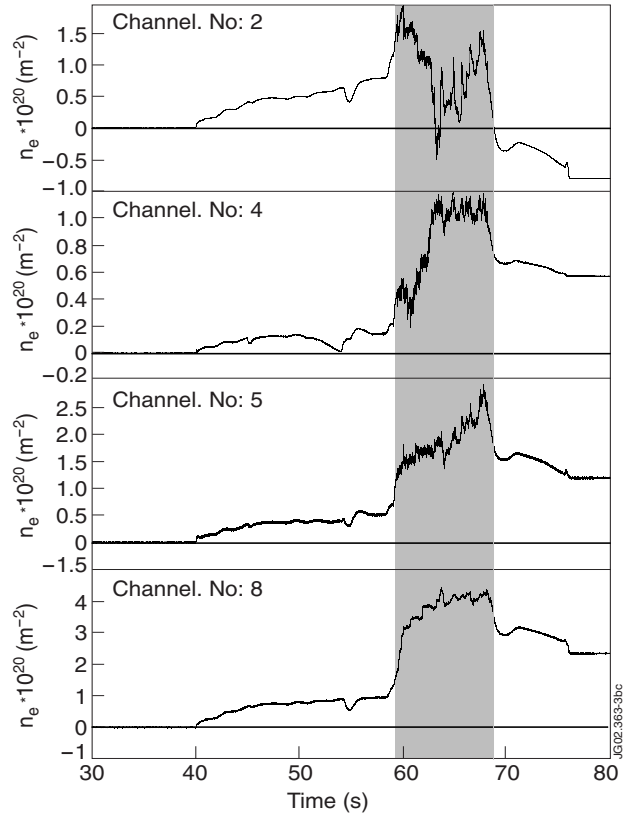


Figure 3b: Pulse No: 52847: Electron line integral measurements on channels #2, #4, #5, #8.

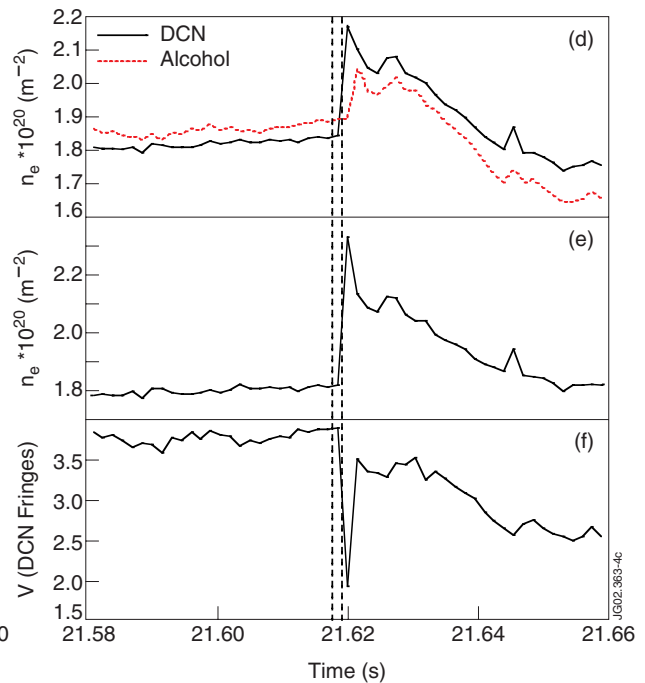
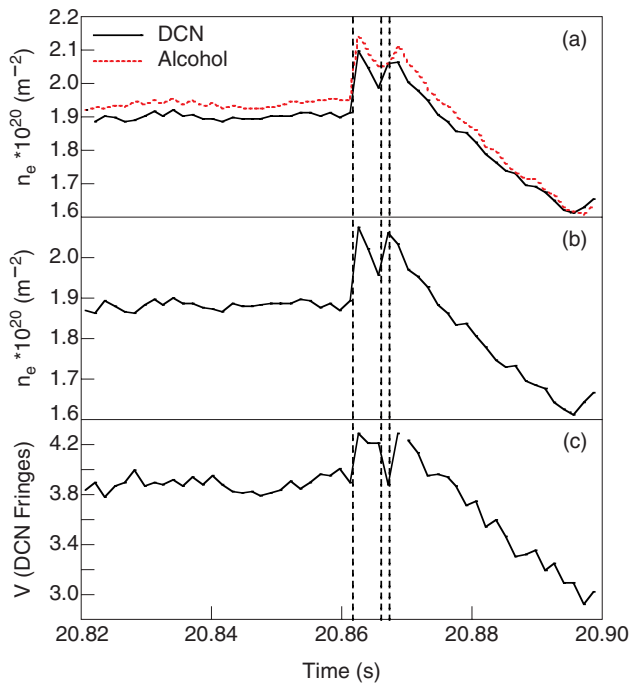


Figure 4: Pulse No: 52842: Line density and vibration measurements without fringe correction. (a,d) Measured line density by the DCN and Alcohol laser. (b,e) Computed line integrated density. (c,f) Computed normalised vibration amplitude. The dashed lines shown the fringe jumps times.

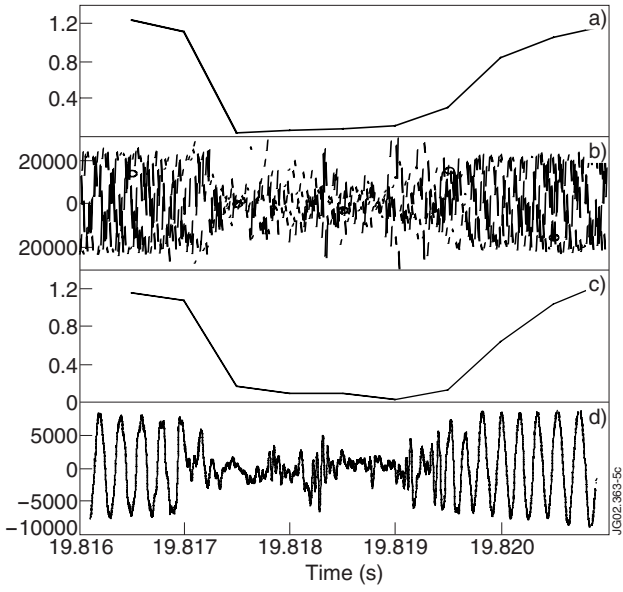


Figure 5: Pulse No: 52844, channel #5: (a) DCN signal amplitude computed by VME system. (b) Fast sampled DCN signal. (c) Alcohol signal amplitude computed by VME system. (d) Fast sampled Alcohol signal.

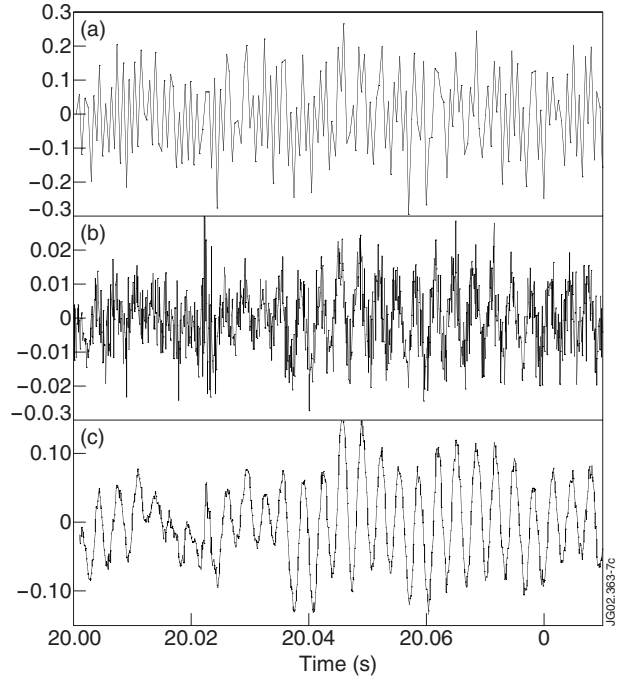


Figure 7: Pulse No: 52863, channel #5: (a) computed by the VME system, (b) computed from the fast sampled signals with 0.1 ms delay, (c) computed from the fast sampled signals with 1 ms delay.

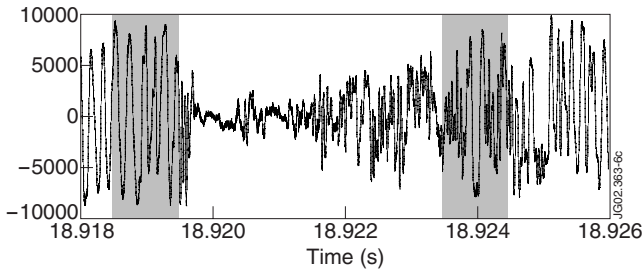


Figure 6: Pulse No: 52863, channel #5: Fast sampled Alcohol signal.

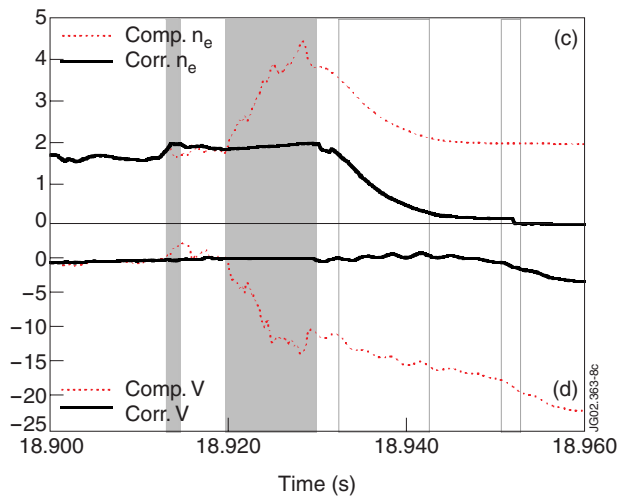
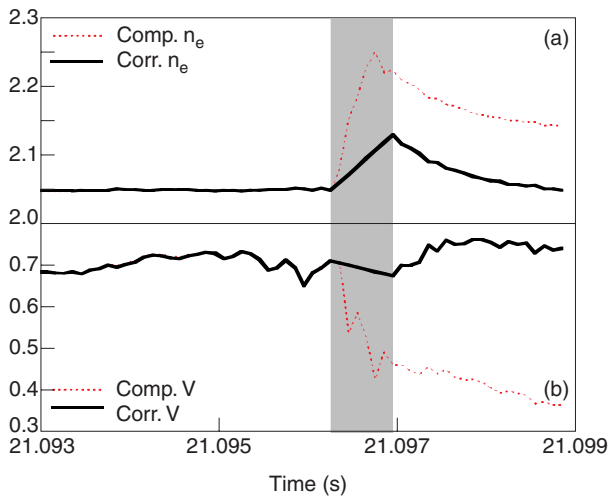


Figure 8: Computed and correct density (a) and vibration (b) for Pulse No: 52859 with an ELM event. Computed and correct density (c) and vibration (d) for Pulse No: 52863 with a disruption event.